Chemistry & Biology, Vol. 9, 321–332, March, 2002, ©2002 Elsevier Science Ltd. All rights reserved. PII S1074-5521(02)00117-5

Heme-Artemisinin Adducts Are Crucial Mediators of the Ability of Artemisinin to Inhibit Heme Polymerization

R. Kannan, Dinkar Sahal, and V.S. Chauhan[1]
Malaria Group
International Centre for Genetic Engineering and Biotechnology
Aruna Asaf Ali Marg
New Delhi 110 067
India

Summary

A lack of molecular understanding of the targets and mechanisms of artemisinin action has impeded the improvisation of more efficient antimalarials based on this class of endoperoxide drugs. We have synthesized a heme-artemisinin adduct designated as "hemart" to discover if it mediates the ability of artemisinin to inhibit heme polymerization. Hemart mimics heme in binding to *Plasmodium falciparum* histidine-rich protein II (PfHRP II) but cannot self-polymerize. Instead, it inhibits all heme polymerizations, including basal and those triggered by PfHRP II, Monooleoyl glycerol (MOG), or *P. yoelii* extract. Hemart has an edge over heme in displacing heme from PfHRP II, and either low pH or chloroquine dissociates heme but not hemart from PfHRP II. Our results suggest that hemart, by mimicking heme, stalls all mechanisms of heme polymerization, resulting in the death of the malaria parasite.

Introduction

Malaria in its present incarnation poses an alarming threat to mankind because the quinoline-based drugs that were icons of assurance until some time ago are being increasingly tamed by the plasmodium's evolving biochemical machinery [1, 2]. On one hand, there is a dearth of new antimalarials, and on the other there is a lack of comprehensive understanding of how the existing antimalarials act or how they are rendered ineffective. These lacunae have been responsible for giving the impression that chemotherapy may be losing its war against the malaria parasite. Because most antimalarials target the blood stages of the parasite [3], a proper perspective of the infected red blood cell is essential for understanding drug action. It is in this stage that the parasite, through a process of sequential proteolytic degradation in the food vacuole, utilizes the host hemoglobin as a major source of amino acids [4]. Degradation of hemoglobin is accompanied by release of the toxic free heme, which is detoxified by a heme polymerization pathway unique to the parasite. The polymerized heme accumulates in the form of an insoluble, microcrystalline, redox-inactive iron (III) black-brown heme pigment called hemozoin or the malaria pigment. Because this heme polymerization pathway is unique to the parasite, it offers an attractive target for the design of new antimalarials [5]. The structure [6] and genesis [7] of hemozoin are topics of contemporary interest because many antimalarial drugs, including chloroquine [8] and artemisinin [9], are known to antagonize the heme polymerization pathway.

The malaria parasite produces a series of histidine-rich proteins (HRP II, 31.7 kDa; HRP III, 22.3 kDa; and HRP IV, 10.6 kDa). Of these, the former two are known to bind multiple heme monomers and are thought to be instrumental in heme detoxification [10]. Our earlier work involving heme binding studies with synthetic peptides representing the repetitive hexapeptide sequence (AHHAAD) in *Plasmodium falciparum* histidine-rich protein II (PfHRP II) suggests these to be the binding sites for heme [11]. Mere binding of multiple hemes by a histidine-rich polypeptide (e.g., polyhistidine) is not enough to enable heme polymerization into hemozoin. Conformational requirements of the protein template that catalyzes heme polymerization appear to be necessary because PfHRP II that has been heat inactivated by boiling fails to catalyze heme polymerization [10]. A dendrimer of AHHAAD sequences has been shown to catalyze heme polymerization [12], suggesting its ability to organize the inter-heme proximity relations that may facilitate heme polymerization. Although histidine-rich proteins of the parasite appear to be attractive catalysts of heme polymerization, some evidence points to the possibility of alternate mechanisms that the parasite may adopt to cause the same. These include the ability of acetonitrile or chloroform extracts of the parasite to cause heme polymerization [13, 14] and the successful parasitism shown by PfHRP II and III knockout variants of the malaria parasite [15, 16]. In view of the multiplicity of heme polymerization mechanisms seen in the malaria parasite, those drugs that target several of the crucial mechanisms are likely to be more potent than the ones that target only a few of these mechanisms.

Among the few drugs against malaria, the most promising, from considerations of potency and efficacy, is artemisinin, an endoperoxide molecule derived from an ancient Chinese herbal remedy, Quinghaosu. Artemisinin has rapid onset of action with parasite clearance from the blood within 48 hr in most cases [17]. The blood stage parasite is sensitive to nM concentrations of artemisinin, whereas its toxicity to normal erythrocytes becomes evident only at μM concentrations [18]. Artemisinin and its hemisynthetic derivative artmether are currently used to treat severe or multidrug-resistant *Plasmodium falciparum* malaria, including cerebral malaria [19]. Inspite of an attractive drug profile for artemisinin and its analogs, our knowledge of the molecular mechanisms of action of this class of drugs is in its infancy [20]. The presence of the endoperoxide bridge in artemisinin is crucial because analogs lacking this moiety are inactive [21, 22]. Peroxides are well known to decompose into free radicals in the presence of iron [23], and the malaria parasite has long been suspected of being vulnerable to free radicals [24]. Furthermore, free-radical

[1]Correspondence: virander@icgeb.res.in

scavengers inhibit artemisinin's antimalarial activity, and high oxygen tension and other free-radical generators promote it [25–27]. Interestingly, in artemisinin the endoperoxide per se is quite inert, and in the absence of iron, artemisinin has little or no oxidizing or alkylating ability. The oxidizing effects of artemisinin on cells are greatly enhanced in the presence of heme [28, 29]. Besides, iron chelators are known to antagonize the antimalarial and acute toxic effects of the drug [25–27]. Computer-assisted studies have suggested that in the most stable docked configuration, the endoperoxide bridge is in close proximity to the heme iron [30]. In this and a subsequent quantitative structure-activity relations (QSAR) study [31], heme has been proposed to act as a receptor for artemisinin. Recent studies have shown that artemisinin taken up by the malaria parasite growing in vitro was selectively concentrated in the parasite food vacuole, where it was associated with hemozoin [32]. This suggests that artemisinin and heme recognize each other [33], and the intermolecular recognition between the two may not only generate free radicals but may also prejudice them by proximity into alkylating heme rather than any other exogenous biomolecule. Indeed, it was found that artemisinin forms covalent adducts with heme when incubated in a cell-free system and that these adducts of heme and artemisinin are also formed in artemisinin-treated parasites [32]. Robert and Meunier [34] have elucidated the first NMR structure of an artemisinin-porphyrin adduct that results from a C-alkylation of the porphyrin cycle by a radical produced by reductive homolytic cleavage of the peroxide bridge of artemisinin. However, the mechanism by which alkylated heme kills the parasite is not known.

Our experiments suggest that heme-artemisinin adducts mimic heme and inhibit all modes of heme polymerization in the crude parasite extract. More specifically, we have found that hemart inhibits basal heme polymerization and polymerizations catalyzed by PfHRP II or 1-monooleoyl-rac-glycerol (MOG). In the absence of heme polymerization, the resulting build-up of free heme to fatally high concentrations could be one of the mechanisms by which heme-artemisinin adducts kill the parasite.

Results

Synthesis, Purification, and Structural Characterization of Heme-Artemisinin Adducts

To study the reaction between hemin and artemisinin, we dissolved the two in dimethyl acetamide (DMA) and carried out the reaction as described in the Experimental Procedures. Under these conditions the two were highly soluble, allowing us to carry out the reaction at a concentration of 200 mM. As shown in Figure 1, the reaction gave a high yield (typically >50%) of a purified single adduct (hemart II).

We started our investigations by a structural characterization of hemart in comparison with its two constituents, namely hemin and artemisinin, respectively. A comparison of the chromatographic and spectroscopic characteristics of the three is shown in Table 1. The longer RPHPLC retention time of hemart II suggests it

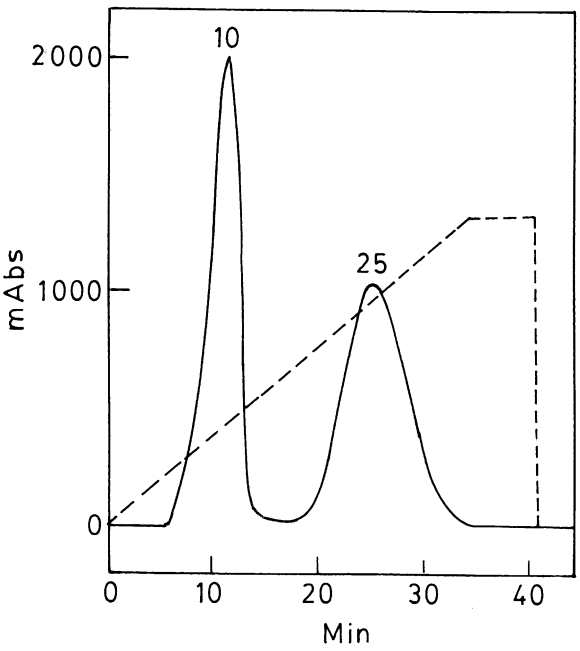

Figure 1. RPHPLC Profile of the Reaction Mixture of Hemin and Artemisinin in DMA

A microbondapak C 18 column (7.8 × 300 mm) was used at a flow rate of 2 ml/min. The gradient used was 30% acetonitrile, 0.1% trifluoroacetic acid (tfa) to 37% acetonitrile, and 0.1% tfa over 35 min. The detector was tuned at 400 nm. The peaks at 10 and 25 min represent hemin and hemart, respectively.

to be more nonpolar than hemin. Indeed, in solvents such as benzene and ethylacetate, hemart is considerably more soluble than hemin. Hemart showed a more red-shifted λ_{max} than hemin. IR spectra suggested that the lactone and the peroxide, which characterize artemisinin [35], were absent in hemart. Unlike hemin, which is optically inactive, hemart showed a circular dichroism at 407 nm. Both hemin and hemart were found to show a bathochromic shift upon the addition of dithionite, suggesting that the oxidation state of iron in both was 3^+. The estimated molar extinction coefficients ($M^{-1}\cdot cm^{-1}$) of heme and hemart in 0.01 N NaOH were nearly equal at 62,000 for heme and 58,000 for hemart (Table 1). A value of 58,000 $M^{-1}\cdot cm^{-1}$ has earlier been reported for heme [36]. The binding of heme to PfHRP II increased its molar extinction coefficient ($M^{-1}\cdot cm^{-1}$) from 62,000 to 66,100. However, the molar extinction coefficient of PfHRP II bound hemart showed a minor drop, from 58,000 to 56,700 $M^{-1}\cdot cm^{-1}$ (Table 1).

Hemart Mimics Heme and Binds PfHRP II at Multiple Sites

Native Gel Electrophoresis to Monitor Binding of Heme/Hemart to PfHRP II

Figure 2 shows the native gel electrophoresis of heme-PfHRP II and hemart-PfHRP II complexes, respectively. Unlike free PfHRP II, which gave two sharp Coomassie bands, the lanes corresponding to heme-PfHRP II complexes showed a diffuse pattern of Coomassie staining. In contrast, the Coomassie staining of hemart-PfHRP II complexes showed two sharp bands at positions slightly

Table 1. Spectroscopic and Chromatographic Characterization of Hemin, Artemisinin, and Hemarts

	Hemin	Artemisinin	[a]Hemart
Visible Spectrum			
(λ_{max} in DMSO), nm	398	colorless	407
IR Spectrum[b]			
Lactone (1734 cm^{-1})	−	+	−
Peroxide (882 cm^{-1})	−	+	−
ESMS	652	282	856 (hemart I) 838 (hemart II)
Oxidation state of iron	3+	N/A	3+
CD spectrum	nil	not done	Positive ellipticity at 407 nm
RPHPLC			
[c]Retention time (min)	10	not done	18 (hemart I) 25 (hemart II)
Molar extinction coefficient (M^{-1} cm^{-1})			
Solvent			
(a) 0.01 N NaOH	62,000 (383)[d]		58,000 (404)
(b) HRP II in 200 mM HEPES (pH 7)	66,100 (413)	colorless	56,700 (423)

[a] Hemart refers to hemart I except where indicated otherwise.
[b] [35].
[c] RPHPLC was done on a microbondapak (Waters) C18 column (7.8 × 300 mm). Flow: 2 ml·min^{-1}. The gradient used was 30% acetonitrile, 0.1% TFA to 37% acetonitrile, and 0.1% TFA over 35 min. Detector: 400 nm.
[d] Values in parentheses represent the wavelengths (nm) at which the molar extinction coefficients were determined.

ahead of the corresponding free PfHRP II bands. In order to find out if the protein bands seen in Coomassie staining represented their complexes with heme/hemart, we ran an identical gel and stained it for peroxidase activity. We saw a direct correspondence between the patterns of Coomassie and peroxidase stains. Thus, the diffuse trailing pattern for heme-PfHRP II complexes and the sharper band pattern seen in the Coomassie stain of hemart-PfHRP II complexes were exactly reflected in the peroxidase stain. These results of staining exclusively for protein or for heme/hemart clearly suggest that, quite like heme, hemart also binds PfHRP II.

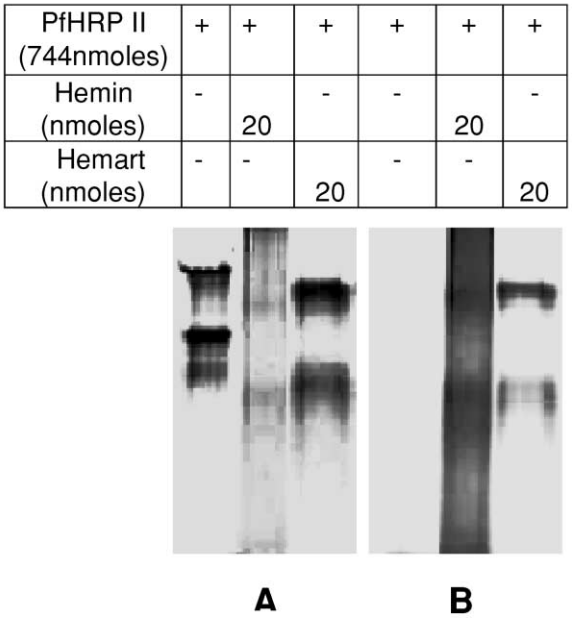

Figure 2. Native PAGE Analysis of Binding of Heme/Hemart to PfHRP II

(A) Coomassie stain.
(B) Peroxidase stain.

Difference Spectroscopy to Titrate Number of Heme/Hemart Binding Sites on PfHRP II

Free heme and free hemart in HEPES buffer (pH 7) show λ_{max} at 382 nm and 406 nm, respectively. Figure 3 shows the results of the difference spectra recorded for the PfHRP II complexes of the two ligands. Binding of heme with PfHRP II shifts the λ_{max} of heme to 415 nm. Whereas the soret band at 415 nm is sharp, the pq bands have two local maxima at 535 nm and 558 nm, respectively (Figure 3A). A plot of this data in the format shown in Figure 3C suggests that at pH 7 approximately 50 molecules of heme bind per monomer of PfHRP II. This is consistent with a previous report [37]. The results of a similar binding study done with hemart are shown in Figure 3B. A distinct soret band can be seen at a characteristic λ_{max} of 426 nm. The pq region of the spectrum shows a single local maximum centered at 550 nm. A plot of this data in the format shown in Figure 3C suggests that at pH 7 approximately 30 molecules of hemart bind per monomer of PfHRP II.

Hemart Displaces Heme from PfHRP II

We exploited the characteristically different λ_{max} values associated with heme-PfHRP II versus hemart-PfHRP II complexes to find out if hemart and heme can displace each other from their binding sites in PfHRP II. As shown in Figure 4A, the addition of progressively increasing amounts of hemart to a saturated heme-PfHRP II complex caused a progressive red shift from 415 nm to 426 nm, suggesting a substitution of heme by hemart in the ligand binding sites of PfHRP II. It may also be noted that the dual local maxima at 535 and 558 nm, respectively, characteristic of heme-PfHRP II, gave way to a single local maximum at 550 nm, characteristic of the hemart-PfHRP II complex. The intermediate wavelengths between 415 nm and 426 nm apparently represent mixed complexes of PfHRP II with both heme and hemart,

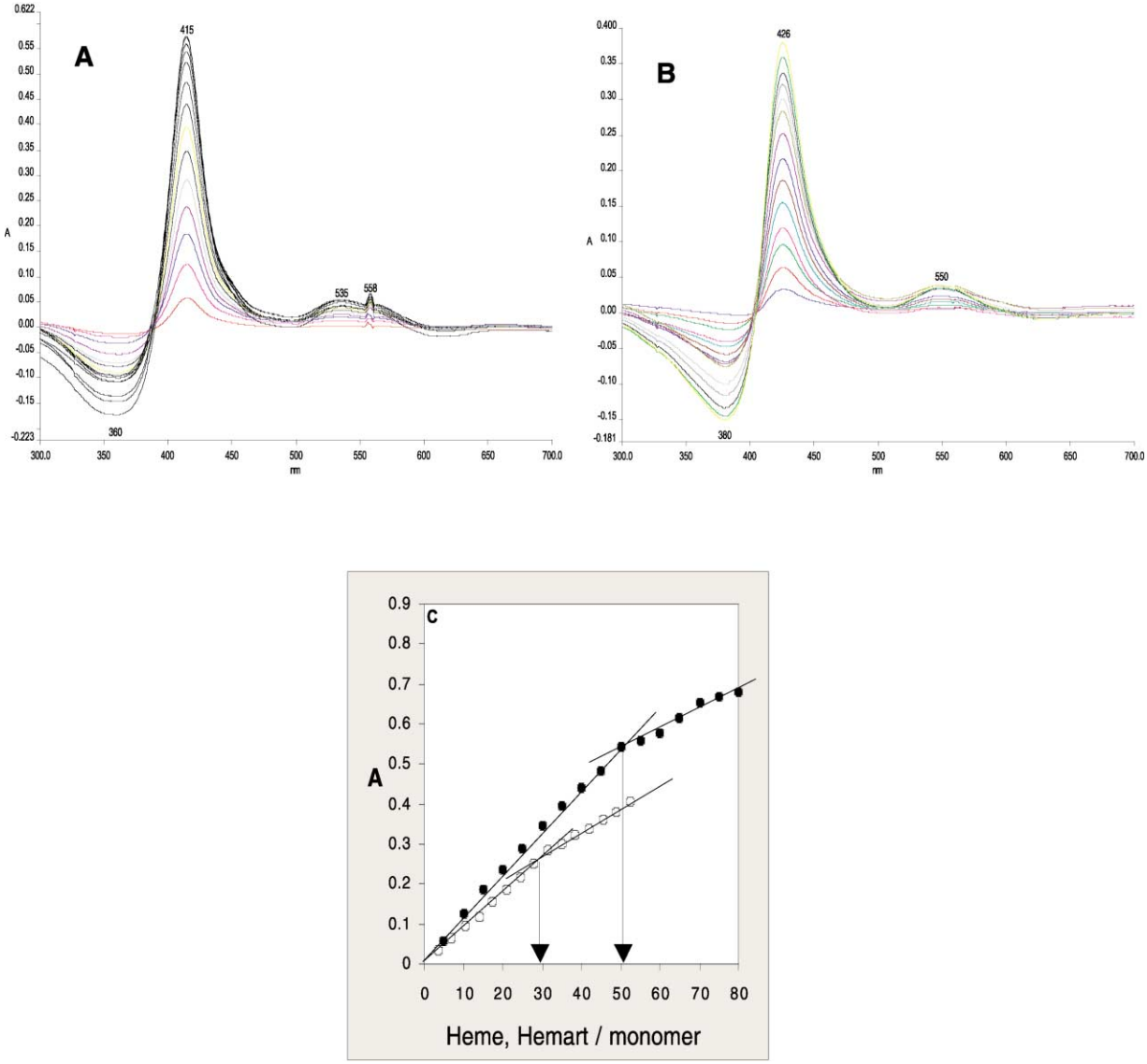

Figure 3. Difference Spectroscopic Titration

Heme (A) and hemart (B) binding to PfHRP II was studied at pH 7 as described in the Experimental Procedures. Transformation of the binding data (C) to show the number of binding sites per molecule of PfHRP II is shown for heme (filled circles) and hemart (open circles), respectively.

respectively. Figure 4B shows the relationship between the concentration of hemart and the change in λ_{max}. The IC_{50} value of this experiment suggests that the apparent binding constant of PfHRP II for hemart is approximately 30 μM. On the other hand, when a hemart-saturated solution of PfHRP II was titrated with progressively increasing amounts of heme, we observed that heme up to a concentration of 150 μM was unable to dissociate and replace hemart from its PfHRP II complex (Figure 4A, inset).

Chloroquine Abrogates Heme-PfHRP II Interactions but Has No Effect on Hemart-PfHRP II Interactions

Because heme was unable to displace hemart from PfHRP II, we wondered if hemart-PfHRP II interactions were qualitatively different from heme-PfHRP II interactions. In an earlier study, we showed that chloroquine disrupts heme-PfHRP II complex [38]. We used chloroquine as a probe to inquire if the molecular nature of interactions between heme versus hemart and PfHRP II was same or different. As shown in Figure 5A, progressive additions of chloroquine to the heme-PfHRP II complex led to a progressive decline in the absorbance intensity at 415 nm. This was suggestive of the ability of chloroquine to dissociate heme from PfHRP II. In contrast, progressive additions of chloroquine to hemart-saturated PfHRP II solution (Figure 5B) caused no significant change in the absorbance intensity at 426 nm. This suggested that, unlike heme, hemart cannot be displaced by chloroquine from its state of complexation with PfHRP II. Figure 5C shows the concentration-

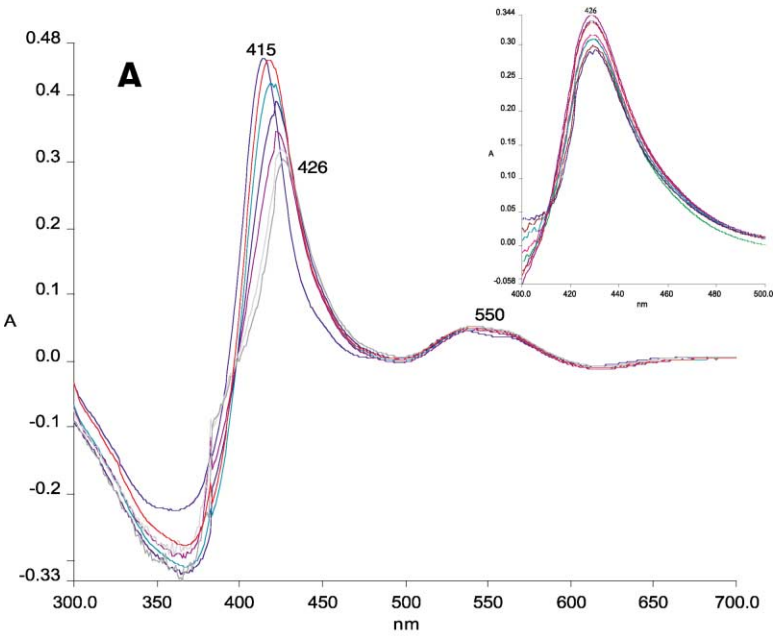

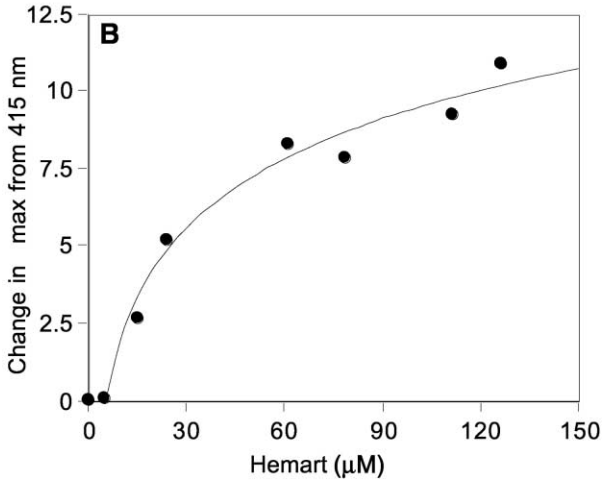

Figure 4. Displacement of Heme from Heme-PfHRP II by Hemart

A heme-saturated PfHRP II sample in HEPES buffer (100 mM, pH 7) was titrated with increasing amounts of hemart. The experiment (A) was done in a difference spectrum mode. The titration starts from heme alone bound to PfHRP II at the λ_{max} centered at 415 nm. The progressive shifts from 415 nm to 426 nm represent progressive displacement by hemart of heme bound to PfHRP II. The end point of the titration is centered at 426 nm. The inset shows that in the case of hemart-saturated PfHRP II, when analogous titration is done with progressively increasing concentrations of heme (0–150 μM), the λ_{max} remains invariant at 426 nm. Panel (B) shows that the concentration of hemart required for taking the protein-ligands complex to the midpoint of the titration is approximately 30 μM.

dependent specificity with which chloroquine selectively dissociates heme but not hemart from PfHRP II.

Hemart Inhibits Heme Polymerization

Artemisinin has been reported to be a potent inhibitor of heme polymerization [9]. The polymerization of heme in plasmodium is a process in which the histidine-rich proteins or the lipids of the parasite facilitate heme polymerization into hemozoin. In order to find out if hemart by virtue of binding to PfHRP II can inhibit heme polymerization, we studied the effect of different concentrations of hemart on the PfHRP II-catalyzed yield of hemozoin (Figure 6B). We were also interested in asking if hemart-mediated inhibition is intrinsic to the fundamental organization of heme units in hemozoin or is manifested only in protein template mediated heme polymerization. Therefore, we also measured the effect of hemart on basal-unassisted heme polymerization (Figure 6A). To do this, we added increasing amounts of hemart to heme +/− PfHRP II under conditions of heme polymerization and estimated the amount of hemozoin formed. The results suggest that hemart in the total absence of artemisinin acts as a potent inhibitor of both basal and PfHRP II-catalyzed heme polymerization. When artemisinin was comparatively examined as an inhibitor of heme polymerization, it was found to be approximately 3-fold less potent an inhibitor than hemart.

In order to discover if hemart is a specific inhibitor of basal- and PfHRP II-mediated heme polymerization or if its inhibitory potential is more widespread, we also examined the effect of hemart on the ability of lipid to promote heme polymerization. We chose 1-monooleoyl-rac-glycerol (MOG) as a model lipid because it has earlier been shown to have the highest potency among lipids as a facilitator of heme polymerization [14]. As shown

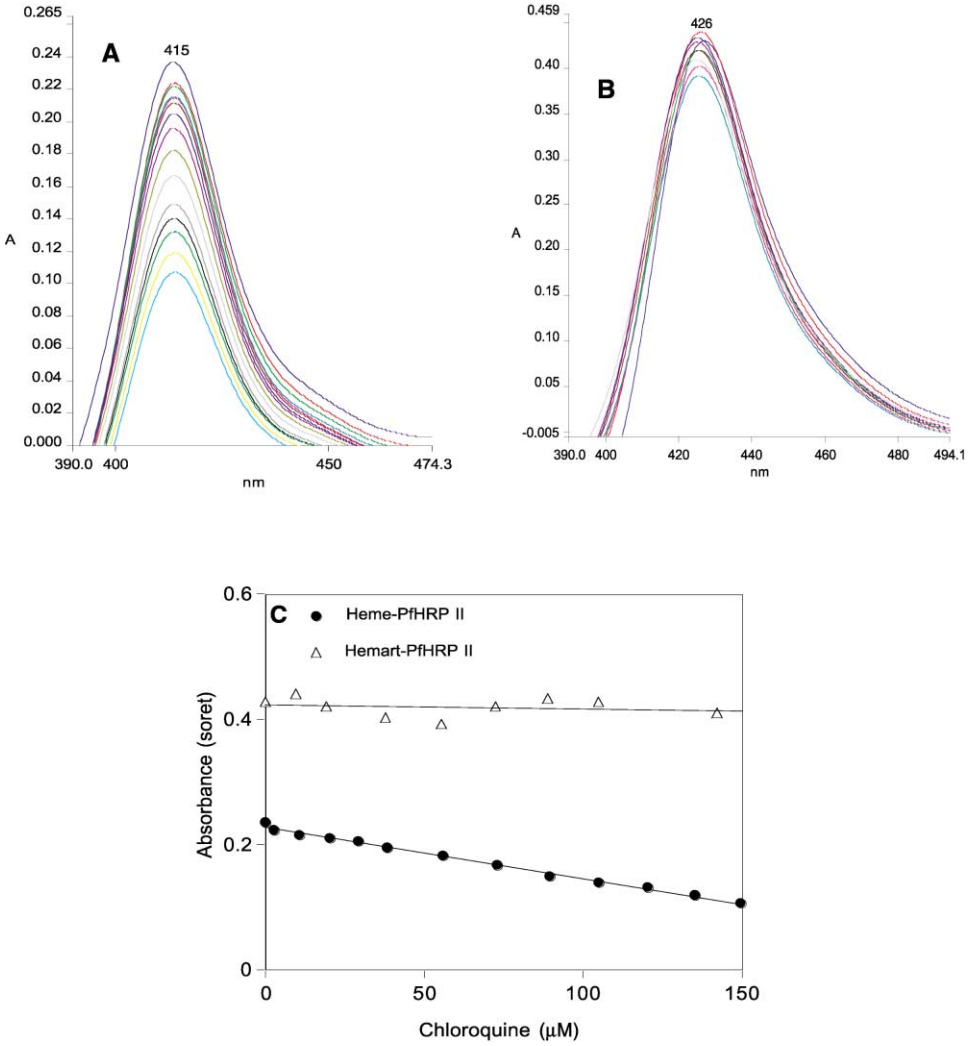

Figure 5. Chloroquine Distinguishes the Heme-PfHRP II Complex from the Hemart-PfHRP II Complex

Influence of chloroquine on the two complexes was studied in the difference spectroscopy mode. In the sample cuvette, PfHRP II (5.9 μg/10 μl acetate buffer, 20 mM [pH 5.5]) was added to 1 ml of HEPES buffer (100 mM, pH 7). Chloroquine diphosphate (stock solution in HEPES buffer [pH 7]) was added in the desired doses to both cuvettes, mixed well, and incubated for 5 min before the difference spectra were recorded.

(A) A decrease in intensity of the heme-PfHRP II soret band as a function of increasing concentrations of chloroquine is shown.

(B) Chloroquine in the same concentration regime as that in (A) is unable to influence the soret band intensity of the hemart-PfHRP II complex.

(C) A plot of change in the soret intensities of the two complexes as a function of increasing concentrations of chloroquine is shown. The IC_{50} value of chloroquine-mediated displacement of heme from PfHRP II is approximately 130 μM.

in Figure 7A, hemart shows complete inhibition of MOG-catalyzed heme polymerization. Because there could be heme polymerization mechanisms other than those that have been explored, we decided to examine the effect of hemart on the heme polymerization ability of the cell-free malaria parasite extract. As shown in Figure 7B, hemart demonstrated its ability to inhibit heme polymerization activity of the malaria parasite extract.

Discussion

Current literature on the mechanism of the antimalarial action of artemisinin is largely empirical. Its identified actions include inhibition of the proteolytic degradation of hemoglobin [9], inhibition of heme polymerization [9], and selective alkylation of some proteins of the parasite [39]. Interestingly, almost all antimalarial effects of artemisinin are strongly accentuated by the presence of heme, suggesting that this endogenous end product of hemoglobin degradation is central to the mechanism of action of artemisinin. More specifically, heme undergoes a chemical reaction with artemisinin to form the heme-artemisinin adducts described by Meshnick and coworkers [32] and in the present work. Here we have investigated whether hemart actuates the ability of artemisinin to inhibit heme polymerization.

We chose DMA as a solvent for the preparation of hemart because both hemin and artemisinin are highly soluble in it. We observed the formation of only one adduct, designated as hemart II (838 Da), which when

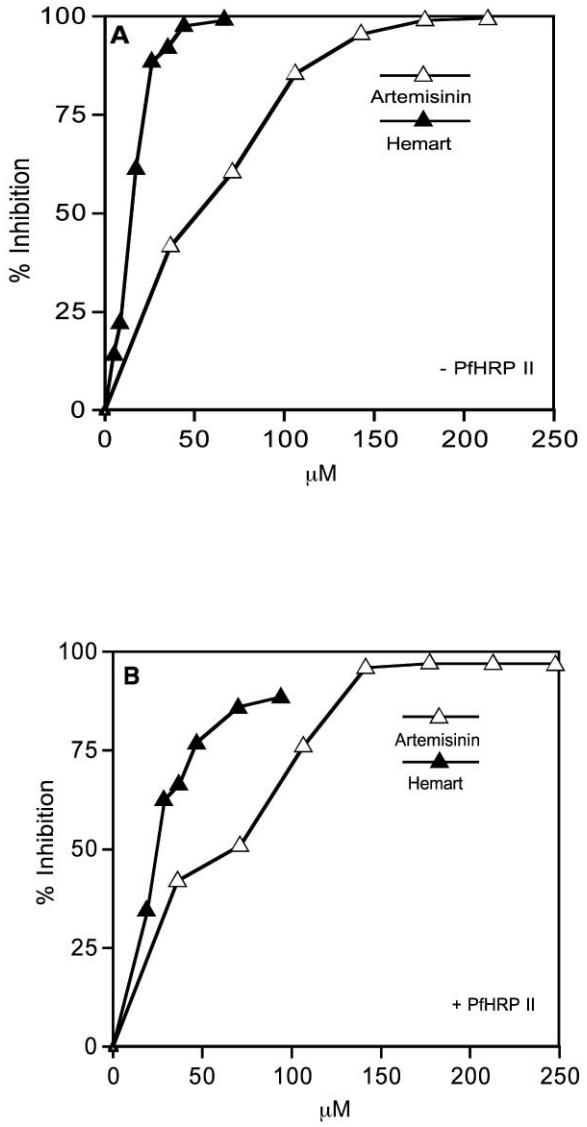

Figure 6. Hemart Is a More Potent Inhibitor of Heme Polymerization Than Artemisinin

The results of inhibition of heme polymerization as obtained in the absence and presence of PfHRP II, respectively. Heme polymerization and hemozoin estimation were done as described in the Experimental Procedures. The IC_{50} values (μM) for hemart and artemisinin in the absence of PfHRP II are 14 and 50, respectively (A). These values in the presence of PfHRP II are 25 and 67, respectively (B). Standard deviations of three independent observations are contained within the points.

incubated with dilute alkali was converted to hemart I (856 Da). The designation of the two hemarts as I and II is based on their early and late retention times, respectively, in RPHPLC (Table 1). It may be of interest that the yield of purified hemart was much higher (approximately 50%) in the present study than the earlier yield (approximately 10%) reported by Yu-Long Hong et al. [32], who carried out the reaction in aqueous methanol.

The purified hemart eluted as a sharp, single peak in RPHPLC. Infrared spectra suggested the absence of peroxide and lactone in hemart. A red shift in the soret frequency of hemart vis à vis heme suggests a change toward a saddle or ruffle in the conformation of the porphyrin (K.M. Smith, personal communication). The presence of iron in hemart is indicated by both peroxidase staining and the sensitivity of the soret band to the addition of dithionite. The observation of a CD absorbance in hemart but not in hemin (Table 1) also suggests that hemin loses its planarity upon conversion to hemart. Proton NMR spectra of heme/hemart in deuterated pyridine with traces of stannous chloride [41] indicated that the downfield meso protons of heme that appear as singlets at 9.93, 10.09, 10.26, and 10.33 ppm are highly reduced in the spectrum of hemart. Further new signals present in neither artemisinin nor heme appear in hemart at 9.61, 9.68, 9.80, and 9.90 ppm in the form of a complex multiplet (see supplementary material). This suggests that alkylation by artemisinin does not have a preferentially targeted meso position on heme, as also reported earlier [40]. The loss of peroxide in hemart is consistent with the well-documented path of reaction between heme and artemisinin, in which after iron-catalyzed rupture of the endoperoxide, an oxygen-centered radical forms and in turn gives rise to a carbon 4-centered radical. The latter has been shown to attack the meso positions of heme dimethyl ester [40]. The structure of hemart reported here is in favor of an adduct where, after cleavage of the endoperoxide, the C-4 centered radical of artemisinin [40] alkylates the meso positions of heme.

We first investigated if PfHRP II, known to bind multiple heme monomers [10, 37], would also bind hemart. Results of a gel retardation assay indicated that both of the ligands are capable of binding to PfHRP II. The observed higher mobility of the PfHRP II complexes with heme/hemart as compared to free PfHRP II may be due to the negative charges from propionates present in both the ligands. In comparison to the discrete bands in the hemart-PfHRP II complex, the diffused bands observed with the heme-PfHRP II complex may suggest that binding of PfHRP II is stronger to hemart than to heme. Results of a difference spectroscopy experiment showed that there are approximately 50 binding sites for heme, which is agreement with the earlier work [37]. In comparison to heme, hemart appears to have only approximately 30 binding sites for PfHRP II. The two ligands also showed a characteristic red shift of their λ_{max} upon binding to PfHRP II; heme showed a shift from 382 nm to 415 nm ($\Delta = 33$ nm), and hemart showed a shift from 406 nm to 426 nm ($\Delta = 20$ nm). However, the maximum absorbances for the two ligands at the end point of titration differed, with 0.55 in the case of heme and 0.25 in the case of hemart. This was surprising because the molar extinction coefficients of the two ligands in the free states are nearly equal (Table 1). However, molar extinction coefficients of the heme- and hemart-PfHRP II complexes were different, with 66 $mM^{-1}{\cdot}cm^{-1}$for the heme-PfHRP II complex in comparison with 56.7 $mM^{-1}{\cdot}cm^{-1}$ for the hemart complex. Compared to a 2.2-fold difference in the absorbance spectra of the two ligands (Figure 3), the difference in the molar extinctions of the bound ligands is only 1.16-fold. Furthermore, PfHRP II appears to have 50 hemin binding sites as compared to around 30 binding sites for hemart.

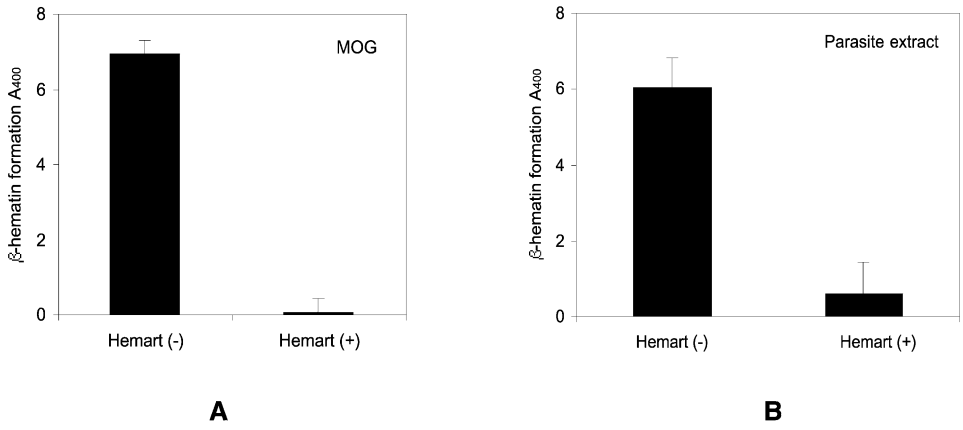

Figure 7. Hemart Inhibits Heme Polymerization Mediated by (A) lipid (MOG) and (B) *Plasmodium yoelii* extract (whole)
The assay was performed as described in the Experimental Procedures. Bars represent standard deviations of three independent observations.

The product of the fold difference in the number of binding sites between hemin and hemart (1.66) and the fold difference in their respective PfHRP II bound molar-extinction coefficients (1.16) is 1.9, which is in close agreement with the 2.2-fold difference of absorbance observed in the difference spectra of the two PfHRP II binding ligands. The reason that PfHRP II apparently binds more heme than hemart monomers could be that the larger surface area of hemart as compared to hemin sterically precludes some binding sites from binding to hemart, and the same feature of hemart may place heme and hemart, respectively, in slightly different microenvironments in PfHRP II. Such a phenomenon can explain (1) how heme and hemart, which have nearly identical molar-extinction coefficients (ϵ) in their free states (Table 1), show significant deviation in ϵ once they bind to PfHRP II and (2) how the aforementioned characteristic shifts in λ_{max} for the two ligands upon binding to PfHRP II are different.

We used the characteristic λ_{max} values of heme-PfHRP II versus hemart-PfHRP II complexes to find out if the two ligands could replace each other from their bound states to PfHRP II. We observed that hemart was able to replace heme from PfHRP II ($IC_{50} \approx 30$ μM) (Figure 4B). Even as the binding of hemart to PfHRP II appears to be only moderately strong, heme at concentrations up to 150 μM was unable to displace hemart from PfHRP II. Likewise, chloroquine, which displaces heme from PfHRP II ($IC_{50} \approx 130$ μM) (Figure 5), failed to show any displacement of hemart from PfHRP II up to a concentration of 135 μM. Also, acid shock with acetic acid (pH 2), which dissociated heme from PfHRP II, failed to dissociate hemart from PfHRP II. It may be noted here that not only is the binding of hemart to PfHRP II stronger than is the case with heme, but hemart also displaces heme from PfHRP II with 4-fold more potency than is the case with chloroquine. The altered properties of hemart vis à vis heme with respect to their interactions with PfHRP II seem to provide clues toward the molecular mechanism of action of artemisinin. The higher potency of hemart in comparison to artemisinin for inhibiting hemozoin formation (Figure 6) also suggests that hemart may be a crucial intermediate involved in the action of artemisinin. Together with its ability to inhibit heme polymerization, the inability of hemart to self-polymerize seems to make artemisinin a potent antimalarial drug. On one hand, hemart, which shares many properties with heme, can itself be toxic to the parasite, and on the other hand its ability to cause accumulation of free heme can cause lethal biochemical perturbations in the parasite.

However, the mechanism by which hemart inhibits heme polymerization is not clear. Polymerization of heme into hemozoin is a well-orchestrated process in which the proper shape, planarity, and size of the heme monomers appear to be of critical importance for the judicious stacking of heme units [42]. Hemart, which represents the alkylation of heme by a bulky polycyclic chiral fragment of artemisinin, may be a strong inhibiting factor of the stacking of heme molecules, which is necessary for heme polymerization [42]. Other possibilities of hemart's actions include drastically changing the conformation of PfHRP II so that the resulting conformation cannot support heme polymerization. The latest model of hemozoin structure shows heme dimers that are formed through reciprocal metaloester bonds to be the units of hemozoin, and a polymer of such dimers is known to result in the formation of hemozoin [6]. Although hemart, with its iron and propionate side chains, like hemin has all the essential requirements to form dimers through reciprocal metaloester bonds analogous to those of heme, the optimum molecular packing characteristic of heme dimers may be seriously hindered in hemart homodimers as well as in heme-hemart heterodimers.

This work's proposed model of artemisinin action (Figure 8) derives credibility from the work by Meshnick and coworkers, who have demonstrated that heme-artemisinin adduct formation does indeed occur in the malaria parasite-infected red blood cell [32]. Based on the high yield of hemart synthesis in an aprotic solvent such as DMA (Figure 1), we propose that the histidine-rich proteins (II and III) by virtue of their ability to bind multiple heme monomers could assist dissolution of the otherwise quite insoluble heme. This way, by solvating heme, the PfHRPs could catalyze the formation of hemart. An

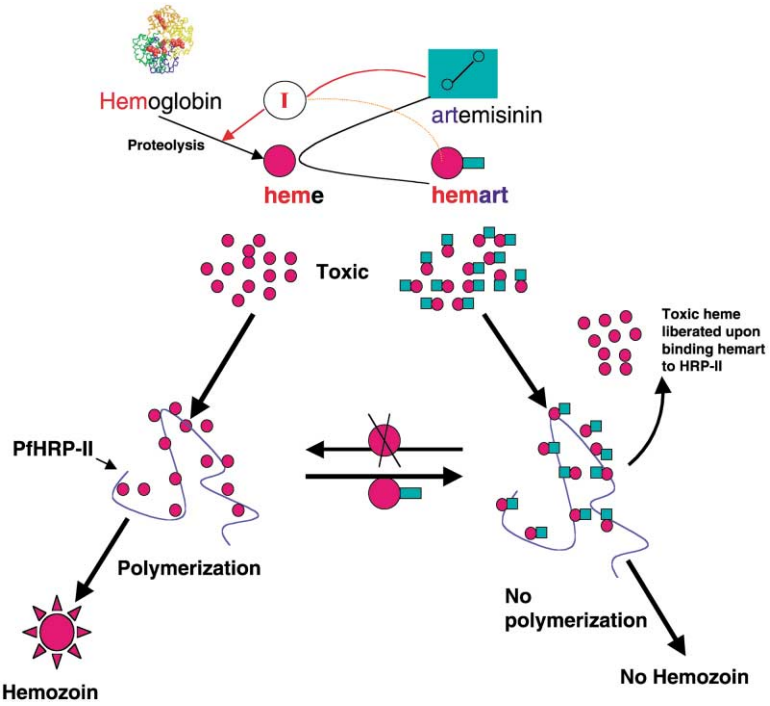

Figure 8. A Model of PfHRP II-Mediated Heme Polymerization and Inhibition of the Same by Artemisinin

Proteolysis of hemoglobin in the food vacuole of the malaria parasite liberates the toxic heme. In the absence of artemisinin, a single molecule of PfHRP II catalyzes several rounds of heme polymerization to hemozoin [10]. In the presence of artemisinin, heme undergoes a reaction with the drug to form hemart. Both heme and hemart are expected to be toxic to the parasite. Compared to heme, hemart exhibits a higher affinity for binding to PfHRP II. Binding of hemart to PfHRP II liberates heme. However, the converse is not true because heme is unable to dissociate hemart from its complex with PfHRP II. As a result, the process of heme polymerization is expected to halt, and the excessive heme/hemart would manifest their toxicity to the parasite. Another target of artemisinin action is the inhibition (I) of proteases that degrade hemoglobin. However, the potency of artemisinin for this effect is markedly increased by the presence of heme [9]. It is possible that the true inhibitor of these proteases may be hemart (orange dotted line).

indication that this may well be the case can be seen in the comparative study of hemart- versus artemisinin-mediated inhibition of heme polymerization in the presence versus the absence of PfHRP II (Figure 6). The hemart-to-artemisinin potency ratio of approximately 3.5 (Figure 6A) in the absence of PfHRP II is reduced to approximately 2.6 in the presence of PfHRP II (Figure 6B). It is likely that the poor bioavailability of heme-artemisinin adducts may be the reason that they fail to show toxicity [32] when presented extracellularly. However, once formed inside the parasite they are likely to be highly toxic, as the model presented in Figure 8 suggests.

Although the major focus of our study has been the manner in which hemart inhibits the PfHRP II-mediated heme polymerization, we have considered the possibility that protein-mediated heme polymerization may not be the only route to hemozoin synthesis in the parasite. We found that hemart also inhibited lipid (MOG)-catalyzed heme polymerization (Figure 7A). Furthermore, we also examined the influence of hemart on the hemozoin formation activity in the whole parasite extract. The observation that hemart inhibits all heme polymerization activities inherent to the malaria parasite (Figure 7B) suggests that the chemical reaction between heme and artemisinin that results in the formation of heme-artemisinin adducts is of crucial importance to the drug action of artemisinin.

In light of recent findings reporting hemozoin formation in the cells of *Scistosoma* [43, 44], it is likely that an antimalarial drug, such as artemisinin, that antagonises heme polymerization may also be effective against Schistosomaisis. A clinical trial using a racemic mixture of α- and β-arteether has been conducted in India [45]. However, in view of our findings reporting the handedness of hemart and its ability to bind PfHRP II, it is imperative to assess if the two diastereoisomers of the resulting hemarts have different binding affinities for PfHRP II. It is not unlikely that the two enantiomers of arteether may have different pharmacological efficacy-to-toxicity ratios, which may make it mandatory to employ only the desired enantiomer in therapy. Furthermore, hemart could act as a lead compound on the basis of whose structure drug design of the future could be rationalized.

Significance

Artemisinin is the drug of choice for chloroquine-resistant and severe cerebral malaria. Inhibition of heme polymerization has been identified as one of the targets of its antimalarial action. However, the molecular details of its action have remained elusive. We have synthesized the hemin-artemisinin adduct (hemart) in excellent yield and have found it to mimic heme in structure and in its ability to bind and displace heme from *Plasmodium falciparum* histidine-rich protein II. First, PfHRP II shows preferential binding of hemart over heme. Second, while heme bound to PfHRP II could be displaced by hemart, heme was unable to displace hemart bound to PfHRP II. The greater affinity of hemart for PfHRP II vis à vis heme is also reflected in the findings that low pH and chloroquine selectively displace heme but not hemart from PfHRP II. Our model of artemisinin action suggests that the displacement of heme as a result of the preferential binding of hemart to PfHRP II could be one of the mechanisms by which artemisinin kills the parasite. Hemart's ability to inhibit heme polymerization is not restricted to the PfHRP II-catalyzed reaction alone because hemart inhibits lipid-catalyzed heme polymerization as well. Finally, the ability of hemart to inhibit heme poly-

merization catalyzed by the whole plasmodium extract testifies to the fundamental role of hemart in inhibiting all modes of heme polymerization adopted by the parasite. We believe that hemart provides us a tool for examining the molecular process of heme polymerization more precisely. Likewise, the structural motif of hemart should give us a lead to the design of more potent antimalarials of the future.

Experimental Procedures

Materials

Artemisinin, chloroquine diphosphate, diaminobenzidine (DAB), dimethyl acetamide (DMA), hemin, 1-monooleoyl-rac-glycerol (MOG), and sodium dodecyl sulfate (SDS) were from Sigma-Aldrich (St. Louis, Missouri, USA). Octadecyl silica (C18, 15–20 μm, 125 Å) used for the purification of hemart was from Waters Millipore corporation, Milford, Massachusetts, USA. Protein estimation was done via the bicinchoninic acid (BCA) method (Pierce, Rockford, Illinois, USA). Hydrogen peroxide was from Merck (Mumbai, India). All other reagents were of analytical grade. Hemin was recrystalized by taking 1 g in 5 ml of pyridine and diluting with 8 ml of chloroform. The solution was then filtered through Whatman filter paper, and the filtrate was added slowly to 70 ml glacial acetic acid containing 1 ml of saturated NaCl and 0.3 ml of concentrated HCl. The resulting solution was heated to 100°C. It was then left undisturbed overnight. Crystals were filtered and washed with 50% acetic acid, alcohol, and ether. The crystallized hemin was then dried over KOH in a vacuum.

Reaction between Hemin and Artemisinin

130 mg (0.2 mmol) of hemin and 56.4 mg (0.2 mmol) of artemisinin were dissolved in 1 ml of DMA and incubated with stirring at 37°C for 24 hr. The reaction mixture was then subjected to reverse-phase chromatography on a glass column with 20 g of C-18 resin preequilibrated with 33% acetonitrile and 0.1% TFA. Chromatographic elution was done by using step gradients in the range of 33%–50% acetonitrile. The column allowed visible separation of hemin (the first to elute) from hemart (eluting last). Hemart was subjected to a rechromatography under the same conditions to remove traces of hemin. Under these conditions the yield (approximately 80 mg) of homogeneous heme-artemisinin adduct was >50%, and only one product, the hemart II (838 Da) was produced. Upon incubation with dilute alkali (0.01 N NaOH, 37°C, 30 min), hemart II was found to be converted to hemart I (856 Da). In all the experiments described in this work, hemart I prepared as described above has been used.

Preparation of Recombinant PfHRP II

The plasmid containing the gene encoding *Plasmodium falciparum* HRP II (PfHRP II) in a pET 3d vector (Novagen, Madison, Wisconsin, USA) was a kind gift from Dr. D.E. Goldberg (Washington University, St. Louis, Missouri, USA). Plasmids were transformed into *E. coli* strain BL 21(DE3). Expression and metal chelate chromatographic purification were done as described previously [10]. Fractions containing PfHRP II were pooled and subjected to desalting on Sephadex G25 (elutent: 20 mM sodium acetate [pH 5.6]). We observed a single band of PfHRP II in reducing SDS polyacrylamide gel electrophoresis (PAGE) and the presence of two dominant bands in nonreducing native or SDS-PAGE. Furthermore, in SDS-PAGE of PfHRP II, as the concentration of β-mercaptoethanol was increased from 0% to 0.1%, the two-band pattern was converted to the higher mobility single-band pattern (data not shown). This seems to suggest that our sample of recombinant PfHRP II had an approximately 1:2 distribution of PfHRP II disulfide dimers and monomers. This possibility is likely in view of the presence of a single cysteinyl residue at the carboxy terminus of recombinant PfHRP II. PfHRP II was estimated by the BCA method with bovine serum albumin (BSA) as a standard. An earlier study [37] has validated the BCA method for accurate estimation of this protein. It was stored at 0.5 mg/ml in aliquots at −20°C. As seen by SDS-PAGE, the protein remained stable for at least one month.

Native PAGE and Peroxidase Staining

Nonreducing, non-SDS, 10% native gel was used. The stacking gel was at pH 6.8, and the resolving gel was at pH 8.8. Samples were diluted into sample buffer containing 10% glycerol, 0.1% bromophenol blue, and 50 mM Tris HCl (pH 6.8) and were loaded without heating. After electrophoresis, all manipulations were done in dark at 25°C. The gel was soaked for 60 min in a 3:7 (v/v) mixture of DAB (6.3 mM in methanol) and acetate buffer (0.25 M, pH 5), respectively. To the above mixture, hydrogen peroxide was added to a final concentration of 30 mM. The gel was incubated for approximately 30 min. When the brown-colored bands showed up with good contrasts, the gel was washed with isopropanol: acetate buffer (3:7 v/v).

Spectroscopic Characterization of Hemin and Hemart

Hemart and hemin were characterized by RPHPLC and by spectroscopic methods. Electron spray mass spectroscopy (ESMS) was done at the National Institute of Immunology in New Delhi, and infrared (IR) spectra were recorded on a Bio-Rad 175C FTIR at the National Physical Laboratory in New Delhi. Visible spectra were recorded on a Hitachi-557 double-beam spectrophotometer. Circular dichroism (CD) spectra were recorded on a Jasco J-720 spectropolarimeter with attached data processor at the central instruments facility at Jawaharlal Nehru University in New Delhi. CD measurements were made by dissolving hemin/hemart in DMSO at a concentration of 0.15 mg/ml. Molar extinction coefficients of rigorously pure free ligands were measured after they were dried in vacuo over KOH to constant weights. These coefficients for the PfHRP II bound ligands were measured after the addition of precisely known trace amounts of the two ligands to excess PfHRP II solution in HEPES buffer (100 mM, pH 7).

Spectroscopic Studies of Heme/Hemart Binding to PfHRP II

Sample Preparation

The stock solutions of heme and hemart were made by dissolving recrystalized hemin and repurified hemart, respectively, in 10 μl of 1 N NaOH and then diluting 100 times with water. The solutions were then filtered through a 0.45 μm syringe filter. Concentrations of these stock solutions were determined spectroscopically by using ϵ_{383} (hemin) = 62 $mM^{-1}\cdot cm^{-1}$ and ϵ_{404} (hemart) = 58 $mM^{-1}\cdot cm^{-1}$.

Spectroscopic Estimation of Binding of Heme/Hemart to PfHRP II

Difference spectroscopic ligand binding titrations were done as described [37]. Solutions of 1 mM hemin/hemart were made in HEPES buffer (100 mM, pH 7) from their respective stocks, and the two ligands were titrated at 27°C for binding to PfHRP II in two separate experiments. The ligand solutions were simultaneously added into the sample cuvette containing 23.8 μg of PfHRP II in 2 ml of 100 mM HEPES buffer (pH 7) and the reference cuvette containing the buffer alone. The ligand solutions were added in 1 μM increments, and difference absorption spectra were recorded after each addition, when solutions were mixed and given 5 min for complete binding. The spectra had their maxima and minima at 415 nm and 360 nm, respectively, for hemin and 426 nm and 380 nm, respectively, for hemart. The heme and hemart binding curves were constructed by plotting A_{415}/A_{426} versus heme/hemart concentrations, respectively.

Dispalcement of Heme from Heme-PfHRP II by Hemart

In the difference spectrum mode at a concentration at which heme had saturated all binding sites in PfHRP II, hemart solution in μM increments was added to both the cuvettes, mixed, and incubated for 5 min. Difference spectra were monitored for change in λ_{max} from 415 nm (heme-PfHRP II complex) to 426 nm (hemart-PfHRP II complex). In the reverse titration, hemart-saturated PfHRP II was analogously mixed with μM increments of heme. The EC_{50} value of heme dispalcement by hemart was used to get an estimate of the affinity constant of hemart binding to PfHRP II.

Displacement of Heme/Hemart Bound to PfHRP II by Chloroquine at Low pH

Chloroquine-mediated dissociation of the heme/hemart-PfHRP II complex was studied by spectroscopy in the difference spectroscopy mode. In another experiment, the distinguishing effect of pH on the binding of heme versus hemart to PfHRP II was studied by acidification (with acetic acid to pH 2) of heme- or hemart-PfHRP II

complexes and subsequent centrifugation. Under these conditions, free heme or free hemart are insoluble, whereas their PfHRP II bound complexes are either soluble (hemart-PfHRP II) or unstable (heme-PfHRP II). The colors of the pellets and supernatants were observed so that the status of binding of the respective ligands could be judged.

Effect of Hemart on Basal and PfHRP II Catalyzed Heme Polymerization

Heme (final concentration, 380 μM) was aliquoted into eppendorf tubes, and hemart was added in different concentrations (20–100 μM). Then PfHRP II (0.5 mg/ml stock in acetate buffer [pH 5.5]) (3 μg; final concentration, 0.09 μM) was added, and finally, the volume was brought to 1 ml with 200 mM acetate buffer at pH 5. Two controls, heme alone (−ve control) and heme + PfHRP II (+ve control), were always run simultaneously. Basal heme polymerization seen in the heme-alone control was typically <10% of the value seen in presence of PfHRP II. This basal value has been subtracted from all measurements of assisted polymerizations. Each assay was set up in triplicate and incubated at 37°C for 6 hr on a rotating shaker (260 rpm). The reaction was stopped by centrifugation at 14,000 g (15 min, 25°C), and the pellets were suspended in 1 ml of 2.5% SDS in phosphate-buffered saline (PBS) and incubated with shaking as above for 1 hr at 37°C, followed by centrifugation as above. The pellets were given two additional SDS washes, as above. The supernatant of the third wash was nearly colorless. The washed pellets were resuspended in 1 ml of 100 mM bicarbonate solution and incubated for 1 hr at 37°C on a rotating shaker (260 rpm). Centrifugation as mentioned above followed. Two additional bicarbonate washes were given as above. The bicarbonate washes are known to remove free heme and nonhemozoin heme oligomers adsorbed to hemozoin [46]. Finally, the pellets were washed with 95% ethanol. For the estimation of hemozoin, the pellets were solubilized in 1 N NaOH (100 μl) and 2.5% SDS (900 μl), and absorbance was measured at 401 nm. After the procedure given above, neither hemart alone nor hemart + PfHRP II showed any tendency to make a hemozoin-like polymer.

Preparation of Malaria Parasite Extract

Plasmodium yoelii nigeriensis, a rodent malaria parasite, was used for infection. The detailed protocol of infection and preparation of parasite extract was as in Pandey et al. [46].

Effect of Hemart on Lipid (MOG) and Parasite Extract-Catalyzed Heme Polymerization

Heme (final concentration, 380 μM) was aliquoted into eppendorf tubes, and hemart was added at a single concentration of 120 μM. MOG (10 μl in methanol; final concentration 2.8 mM) or parasite extract (20 μl) was added, and the volume was brought to 1 ml with 200 mM acetate buffer (pH 5). Incubation, (+ve) and (−ve) controls, and washing until estimation of hemozoin were done as described above.

Supplementary Material

Three supplementary figures showing NMR spectra are available through the Chemistry & Biology Production Department. Please write to chembiol@cell.com for a pdf.

Acknowledgments

We thank Dr.Allan Saul, Dr. D.E. Goldberg, Dr. Anand Ranganathan, Dr. Amit Pandey, and Dr. Andrew Lynn for critical reading of the manuscript and helpful suggestions. We thank Dr. Alka Gupta for infrared studies, Dr. R.A. Vishwakarma for ESMS, and Dr. Andrew Lynn for CD. We thank the Programma Nazionale Di Ricerca Sui Farmaci Area Malattie Orfane of the government of Italy for financial assistance.

Received: August 16, 2001
Revised: November 8, 2001
Accepted: November 29, 2001

References

1. Su, X.Z., Kirkman, L.A., Fujioka, H., and Wellems, T.E. (1997). Complex polymorphisms in an ~330 kDa protein are linked to chloroquine-resistant *Plasmodium falciparum* in southeast Asia and Africa. Cell *91*, 593–603.
2. Fidock, D.A., Nomura, T., Talley, K.A., Cooper, A.R., Dzekunov, M.S., Ferdig, T.M., Ursos, M.L., Sidhu, A.B., Naude, B., Deitsch, W.K., et al. (2000). Mutations in the *Plasmodium falciparum* digestive vacuole transmembrane protein PfCRT and evidence for their role in chloroquine resistance. Mol. Cell *6*, 861–871.
3. Winstanely, P.A., and Breckenridge, A.M. (1987). Currently important antimalarial drugs. Ann. Trop. Med. Parasitol. *81*, 619–627.
4. Goldberg, D.E., Slater, A.F., Beavis, R., Chait, B., Cerami, A., and Henderson, G.B. (1991). Hemoglobin degradation in the human malaria pathogen Plasmodium falciparum: a catabolic pathway initiated by a specific aspartic protease. J. Exp. Med. *173*, 961–969.
5. Pandey, A.V., and Chauhan, V.S. (1998). Heme polymerisation by malarial parasite: a potential target for antimalarial drug development. Curr. Sci. *75*, 911–918.
6. Pagola, S., Stephens, P.W., Bohle, D.S., Kosar, A.D., and Madsen, S.K. (2000). The structure of malaria pigment β-haematin. Nature *404*, 307–310.
7. Egan, T.J., Mavuso, W.W., and Ncokazi, K.K. (2001). The mechanism of β−hematin formation in acetate solution. Parallels between hemozoin formation and biomineralisation processes. Biochemistry *40*, 204–213.
8. Chou, A.C., Chevil, R., and Fitch, C.D. (1980). Ferriprotoporphyrin IX fulfills the criteria for identification as the chloroquine receptor of malarial parasites. Biochemistry *19*, 1543–1549.
9. Pandey, A.V., Tekwani, B.L., Singh, R.L., and Chauhan, V.S. (1999). Artemisinin, an endoperoxide antimalarial, disrupts the hemoglobin catabolism and heme detoxification systems in malarial parasite. J. Biol. Chem. *274*, 19383–19388.
10. Sullivan, D.J., Jr., Gluzman, I.Y., and Goldberg, D.E. (1996). Plasmodium hemozoin formation mediated by histidine-rich proteins. Science *271*, 219–221.
11. Pandey, A.V., Joshi, R., Tekwani, B.L., Singh, R.L., and Chauhan, V.S. (1997). Synthetic peptides corresponding to a repetitive sequence of malarial histidine rich protein bind heme and inhibit hemozoin formation in vitro. Mol. Biochem. Parasitol. *90*, 281–287.
12. Ziegler, J., Chang, R.T., and Wright, D.W. (1999). Multiple-antigenic peptides of Histidine-Rich Protein II of Plasmodium falciparum: dendrimeric biomineralisation templates. J. Am. Chem. Soc. *121*, 2395–2400.
13. Bendrat, K., Berger, B.J., and Cerami, A. (1995). Haem polymerisation in malaria. Nature *378*, 138–139.
14. Fitch, C.D., Cai, G.Z., Chen, Y.F., and Shoemaker, J.D. (1999). Involvement of lipids in ferriprotoporphyrin IX polymerisation in malaria. Biochim. Biophys. Acta *1454*, 31–37.
15. Wellems, T., Walker-Jonah, A., and Panton, L. (1991). Genetic mapping of the chloroquine-resistance locus on Plasmodium falciparum chromosome 7. Proc. Natl. Acad. Sci. USA *88*, 3382–3386.
16. Walker-Jonah, A., Dolan, S., Gwadz, R., Panton, L., and Wellems, T. (1992). An RFLP map of the Plasmodium falciparum genome, recombination rates and favored linkage groups in a genetic cross. Mol. Biochem. Parasitol. *51*, 313–320.
17. van Agtmael, M.A., Eggelte, T.A., and van Boxtel, C.J. (1999). Artemisinin drugs in the treatment of malaria: from medicinal herb to registered medication. Trends Pharmacol. Sci. *20*, 199–205.
18. Meshnick, S.R., Ranz, A., Thomas, A., Xu, C.-M., and Pan, H.-Z. (1991). Artemisinin (qinghaosu): the role of intracellular hemin in its mechanism of antimalarial action. Mol. Biochem. Parasitol. *49*, 181–190.
19. Benoit-Vical, F., Robert, A., and Meunier, B. (2000). In vitro and in vivo potentiation of artemisinin and synthetic endoperoxide antimalarial drugs by metalloporphyrins. Antimicrob. Agents Chemother. *44*, 2836–2841.
20. Meshnick, S.R. (1998) From quinine to qinghaosu: historical

perspectives. In Malaria: Parasite Biology, Pathogenesis & Protection, I.W. Sherman, ed. (Washington, D.C.: ASM Press), pp. 341–353.
21. Brossi, A., Venugopalan, B., Gerpe, L.D., Yeh, H.J.C., Flippen-Anderson, J.L., Buchs, P., Luo, X.-D., Milhous, W., and Peters, W. (1998). Arteether, a new antimalarial drug: synthesis and antimalarial properties. J. Med. Chem. *31*, 645–650.
22. Robert, A., and Meunier, B. (1998). Is alkylation the main mechanism of action of the antimalarial drug artemisinin? Chem. Soc. Rev. *27*, 273–279.
23. Halliwell, B., and Gutteridge, J.M.C. (1989). Free Radicals in Biology and Medicine, 2nd ed. (Oxford, UK: Clarendon Press)
24. Etkin, N.L., and Eaton, J.W. (1975). Malaria-induced oxidant sensitivity. In Erythrocyte Structure and Function, G. Brewer, ed. (New York: Alan R. Liss).
25. Krungkrai, S.R., and Yuthavong, Y. (1987). The antimalarial action on plasmodium falciparum of qinghaosu and artesunate in combination with agents which modulate oxidant stress. Trans. R. Soc. Trop. Med. Hyg. *81*, 710–714.
26. Meshnick, S.R., Tsang, T.W., Lin, F.-B., Pan, H.-Z., Chang, C.-N., Kuypers, F., Chiu, D., and Lubin, B. (1989). Activated oxygen mediates the antimalarial activity of qinghaosu. Prog. Clin. Biol. Res *313*, 95–104.
27. Levander, O.A., Ager, A.L., Jr., Morris, V.C., and May, R.G. (1989). Quinghaosu, dietary vitamin E, selenium, and cod-liver oil. Effect on the susceptibility of mice to the malarial parasite Plasmodium yoelii. Am. J. Clin. Nutr. *50*, 346–352.
28. Berman, P.A., and Adams, P.A. (1997). Artemisinin enhances heme-catalyzed oxidation of lipid membranes. Free Radic. Biol. Med. *22*, 1283–1288.
29. Meshnick, S.R., Yang, Y.-Z., Lima, V., Kuypers, F., Kamchonwongpaisan, S., and Yuthavong, Y. (1993). Iron-dependent free radical generation from the antimalarial agent artemisinin (Quinghaosu). Antimicrob. Agents Chemother. *37*, 1108–1114.
30. Shukla, K.L., Gund, T.M., and Meshnick, S.R. (1995). Molecular modeling studies of the artemisinin (qinghaosu)-hemin interaction: docking between the antimalarial agent and its putative receptor. J. Mol. Graph. *13*, 215–222.
31. Grigorov, M., Weber, J., Tronchet, J.M.J., Jefford, C.W., Milhous, W.K., and Maric, D. (1997). A QSAR study of the antimalarial activity of some synthetic 1,2,4-Trioxanes J. Chem. Inf. Comput. Sci. *37*, 124–130.
32. Hong, Y.-L., Yang, Y.-Z., and Meshnick, S.R. (1994). The interaction of artemisinin with malarial hemozoin. Mol. Biochem. Parasitol. *63*, 121–128.
33. Paitayatat, S., Tarnchompoo, B., Thebtaranonth, Y., and Yuthavong, Y.Y. (1997). Correlation of antimalarial activity of artemisinin derivatives with binding affinity with Ferroprotoporphyrin IX. J. Med. Chem. *40*, 633–638.
34. Robert, A., and Meunier, B. (1997). Characterization of the first covalent adduct between artemisinin and a heme model. J. Am. Chem. Soc. *119*, 5968–5969.
35. Monhaupt, M., Hagemann, H., Perler, J.P., Bill, H., Boukouvalas, J., Rossier, J.C., and Jefford, C.W. (1988). A vibrational study of some 1,2,4-trioxanes. Helv. Chim. Acta *71*, 992–999.
36. Dawson, R.M.C., Elliot, D.C., Elliot, W.H., and Jones, K.M. (1986). Data for Biochemical Research (Oxford, UK: Oxford University Press), pp. 230–231.
37. Choi, C.Y.H., Cerda, J.F., Chu, H.A., Babcock, G.T., and Marletta, M.A. (1999). Spectroscopic characterisation of the heme-binding sites in Plasmodium falciparum Histidine-Rich Protein 2. Biochemistry *38*, 16916–16924.
38. Pandey, A.V., Bisht, H., Babbarwal, V.K., Srivastava, J., Pandey, K.C., and Chauhan, V.S. (2001). Mechanism of malarial haem detoxification inhibition by chloroquine. Biochem. J. *355*, 333–338.
39. Asawamahasakda, W., Ittarat, I., Pu, Y.-M., Ziffer, H., and Meshnick, S.R. (1994). Reaction of antimalarial endoperoxides with specific parasite proteins. Antimicrob. Agents Chemother. *38*, 1854–1858.
40. Robert, A., Cazelles, J., and Meunier, B. (2001). Characterisation of the alkylation product of heme by the antimalarial drug artemisinin. Angew. Chem. Int. Ed. *40*, 1954–1957
41. Osawa, Y., Highet, R.J., Murphy, C.M., Cotter, R.J., and Pohl, L.R. (1989). Formation of heme-derived products by the reaction of ferrous deoxymyoglobin with $BrCCl_3$. J. Am. Chem. Soc. *111*, 4462–4467.
42. Cazelles, J., Camuzat-Dedenis, B., Provot, O., Robert, A., Mayrargue, J., and Meunier, B. (2000). Alkylating properties of synthetic trioxanes related to artemisinin. J. Chem. Soc. [Perkin 1] *1*, 1265–1270.
43. Oliveira, M.F., d'Avila, J.C., Torres, C.R., Oliveira, P.L., Tempone, A.J., Rumjanek, F.D., Braga, C.M., Silva, J.R., Dansa-Petretski, M., Oliveira, M.A., et al. (2000). Haemozoin in Schistosoma mansoni. Mol. Biochem. Parasitol. *111*, 217–221.
44. Chen, M.M., Shi, L., and Sullivan, D.J., Jr. (2001). Haemoproteus and Schistosoma synthesise heme polymers similar to Plasmodium hemozoin and β-hematin. Mol. Biochem. Parasitol. *113*, 1–8.
45. Mohapatra, P.K., Khan, A.M., Prakash, A., Mahanta, J., and Srivastava, V.K. (1996). Effect of arteether alpha/beta on uncomplicated falciparum malaria cases in upper Assam. Ind. J. Med. Res *104*, 284–287.
46. Pandey, A.V., Singh, N., Tekwani, B.L., Puri, S.K., and Chauhan, V.S. (1999). Assay of β-hematin formation by malaria parasite. J. Pharm. Biomed. Anal. *20*, 203–207.